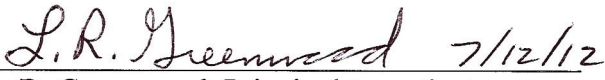# Analysis of AGR-1 Neutron Fluence and Melt Wire Monitors

**July 2012**

**Revision 2**

Pacific Northwest National Laboratory
P.O. Box 999
Richland, Washington 99352
**PNNL Project Number: 58058**

**INL Project 29412, SOW-8802, Rev. 1, 3/14/11**
**MPO 00100467, Amendment 5, 7/6/11**

_L. R. Greenwood_ 7/12/12
L. R. Greenwood, Principal Investigator

_T Trang-le_ 7/12/12
Independent Technical Reviewer

_Deborah Coffey_ 7-12-2012
D. S. Coffey, Quality Engineer

Prepared for

Battelle Energy Alliance, LLC (BEA)
Idaho National Laboratory
P. O. Box 1625
Idaho Falls, ID 83415-1303

# Analysis of AGR-1 Neutron Fluence and Melt Wire Monitors

L. R. Greenwood (Pacific Northwest National Laboratory)

## Summary

The AGR (Advanced Gas Reactor)-1 irradiation was conducted in the Advanced Test Reactor (ATR) at Idaho National Laboratory (INL) during cycles 138B through 145A from December 26, 2006 to November 6, 2009. The assembly was irradiated in the East B10 position of the ATR with a total exposure of 620.2 FPD (full power days at an average power of about 22 MW). Neutron fluence monitors and melt wire monitors were located in all six capsules in the AGR-1. These monitors were previously fabricated at Pacific Northwest National Laboratory (PNNL). After irradiation, the monitors were sent to PNNL for analysis and logged in under Analytical Support Operations (ASO) laboratory Analysis Service Request (ASR) 8934 and assigned sample ID numbers. The neutron fluence monitors were analyzed to determine the activities of the activation products. The measured activation rates were used to adjust the calculated neutron spectra at each of the six capsule locations in the AGR-1 assembly to determine the best fit to the neutron fluence spectra. Melt wire monitors were found for capsules 2, 4, and 6 and it appears that the Be wires melted for capsules 2 and 4. Results are not definite for capsule 6 since no material having the appearance of melted Be could be identified. The melt wire monitors were not recovered for capsules 1, 3, and 5.

The report was previously revised to include additional neutron fluence values which were requested for comparison with calculations at INL. The current revision includes a time-averaged neutron spectrum from INL and takes into account the impact of the low thermal flux during the early cycles of the irradiation history in the Advanced Test Reactor. These changes have very small impact on the thermal and epithermal neutron fluences.

## Preparation of Neutron Fluence and Melt Wire Monitors

In this report the word capsule refers to one of six irradiation capsules comprising the AGR-1 test train, each capsule containing 12 fuel compacts inside a single graphite fuel holder, whereas the word monitor refers to small, encapsulated neutron fluence wires and melt wires previously provided by PNNL. Small wires consisting of very high purity Nb, Fe, and 1% Co-V alloy were encapsulated separately in vanadium tubing measuring 0.05" OD by about 0.3" long for the neutron fluence monitors. Melt wire monitors each contained 2 Be wires. The vanadium tubes had identification codes stamped on the bottom and each wire was accurately weighed. The vanadium tubes were electron beam welded in a vacuum and helium leak tested. The wires were typically 0.04" long and had a diameter of about 0.02". The monitor identification codes and wire weights are listed in Table 1. The complete documentation for the fabrication of the fluence monitors was provided to INL in a report for MPO# 00053058 dated June 2006.

**Table 1.** Neutron Fluence Monitors for AGR-1 (Weight in mg)

| INL Capsule | Nb | | 1% Co-V | | Fe | | Be (2 wires) | |
|---|---|---|---|---|---|---|---|---|
| | Monitor ID | Wt, mg | Monitor ID | Wt, mg | Monitor ID | Wt, mg | Monitor ID | Wt, mg |
| 1 | 18 | 9.869 | 7 | 0.852 | 3 | 7.376 | N | 0.334+0.338 |
| 2 | 7H | 9.237 | H | 0.862 | 6 | 6.477 | H | 0.341+0.357 |
| 3 | VE | 8.975 | V | 0.837 | 2 | 6.494 | 4 | 0.350+0.360 |
| 4 | 87 | 9.587 | B | 0.698 | 7 | 6.441 | X | 0.340+0.341 |
| 5 | RU | 9.251 | K | 0.660 | N | 7.842 | K | 0.350+0.329 |
| 6 | R7 | 9.527 | J | 0.829 | 1 | 7.338 | 6 | 0.341+0.371 |

**Post-Irradiation Analyses**

Following irradiation, the vanadium tubes were retrieved from the AGR-1 assembly at INL and sent to PNNL for analysis. Unfortunately, all of the fluence monitors from capsule 1 were lost in the hot cell at INL. Monitors were retrieved from all of the other capsules. All of the items retrieved from each capsule were initially gamma counted at PNNL to verify the type of fluence monitor. All of the fluence wire monitors were located from capsules 2 through 6 except for the Co-V monitors in capsules 3 and 5. The Be melt wire monitors could not be uniquely identified by gamma counting and these monitors were handled separately as described later in this report.

Because each neutron flux wire was separately encapsulated in vanadium, it was not necessary to open the vanadium tubes prior to gamma counting using procedure, RPG-CMC-450, Rev. 1, *Gamma Energy Analysis (GEA) and Low-Energy Photon Spectrometry (LEPS)*. Each monitor was assigned a unique RPL (Radiochemical Processing Laboratory) sample ID # for tracking purposes. The vanadium has very high purity and the weak activation products do not interfere with the activation products from the flux wires. Gamma absorption corrections are applied to account for the thickness of the vanadium capsules.

Gamma and x-ray counting results are listed in Table 2. Due to significant decay since the end of irradiation in November 2009, the Fe-59 (44.5 day) activities were weak and have higher uncertainties than the other activities. Each flux monitor was counted on a gamma detector calibrated with NIST-traceable standards. Control counts are performed daily when the gamma

spectrometers are in use and background counts are taken at least weekly. Nuclear decay data were taken from the National Nuclear Data Center at Brookhaven National Laboratory.

After gamma counting, the vanadium tubes containing the Nb wires were opened and the wires were removed. The Nb wires were dissolved in an acid mixture of $HNO_3$ and HF and aliquots were mounted on very thin filter paper for x-ray counting using low energy photon spectrometers, which are thin Ge detectors optimized to have high-efficiency and high resolution for x-rays. The analysis procedure used was RPG-CMC-450, Rev. 1, *Gamma Energy Analysis (GEA) and Low-Energy Photon Spectrometry (LEPS)*. The initial gamma count of the Nb wires detected the activity of Nb-94 and this isotope was used to verify the preparation of the x-ray mounts. Table 2 lists the measured $^{93m}Nb$ activities in the samples along with the gamma counting results.

The five neutron activation products that were measureable in these samples are due to three thermal neutron reactions and two fast neutron threshold reactions. The thermal neutron reactions are $^{58}Fe(n,g)^{59}Fe$, $^{59}Co(n,g)^{60}Co$, and $^{93}Nb(n,g)^{94}Nb$ (with subsequent neutron capture to $^{95}Nb$) and the threshold reactions are $^{54}Fe(n,p)^{54}Mn$ and $^{93}Nb(n,n')^{93m}Nb$.

**Table 2.** Measured Activities in Bq/mg at Heights Relative to Core Midplane
(decay corrected to November 6, 2009; 1-sigma uncertainties are listed)

| Capsule | RPL# | $^{54}Mn$ | | RPL# | $^{59}Fe$ | | RPL# | $^{60}Co$ | |
|---|---|---|---|---|---|---|---|---|---|
| 2 | 11-2000 | 6.58E+05 | ±4.2% | 11-2000 | 1.93E+06 | ±26.8% | 11-1999 | 4.64E+07 | ±4.4% |
| 3 | 11-2003 | 7.26E+05 | ±4.2% | 11-2003 | 2.55E+06 | ±22.1% | | * | |
| 4 | 11-2006 | 6.55E+05 | ±3.4% | 11-2006 | 1.98E+06 | ±25.0% | 11-2005 | 5.51E+07 | ±4.4% |
| 5 | 11-2009 | 6.88E+05 | ±4.2% | 11-2009 | 2.13E+06 | ±26.0% | | * | |
| 6 | 11-2012 | 4.59E+05 | ±3.4% | 11-2012 | 1.40E+06 | ±21.0% | 11-2011 | 3.72E+07 | ±1.2% |

*Sample not received for analysis

| Capsule | RPL# | $^{94}Nb$ | | $^{93m}Nb$ | |
|---|---|---|---|---|---|
| 2 | 11-1998 | 4.51E+04 | ±2.4% | 2.11E+06 | ±5.3% |
| 3 | 11-2001 | 4.95E+04 | ±2.4% | 2.37E+06 | ±5.3% |
| 4 | 11-2004 | 4.93E+04 | ±2.4% | 2.27E+06 | ±4.8% |
| 5 | 11-2007 | 4.40E+04 | ±2.4% | 2.21E+06 | ±4.8% |
| 6 | 11-2010 | 3.27E+04 | ±2.5% | 1.66E+06 | ±5.3% |

The saturated reaction rates for the neutron activation reactions were calculated for the measured data in Table 2 by correcting for the decay over the irradiation history, atomic weight, isotopic abundance, neutron burnup, and gamma absorption in each wire. The saturated reaction rate is equal to the product of the average neutron flux times the spectral-averaged neutron activation

cross section for each reaction. The decay during irradiation correction was determined by calculating the growth and decay of each activation product over the entire irradiation history using the BCF computer code. BCF calculates the decay for each time segment of constant flux using the equation $A_i (1 - \exp(-LT_i))$, where $A_i$ is the relative flux for time period $T_i$ and L is the decay constant of each activation product given by $\ln(2)/halflife$. The correction factors are normalized to the time-averaged reactor power and can be renormalized to the full power value for neutron flux values. However, the normalization is irrelevant to the integrated neutron fluence values quoted later in this report. The irradiation history was provided by staff at INL.

Table 3 lists the correction factors that were used to determine the saturated reaction rates. Gamma self-absorption in the wires was calculated from the total photon absorption cross sections given by E. Storm and I. Israel, Nuclear Data Tables, Vol. 7, No. 6, June 1970, and the corrections averaged around 1%. Neutron burnup refers to the depletion of target or product atoms due to neutron absorption. Corrections were applied in an iterative method using the measured reaction rates as the first approximation and iterating until the process converges. The largest correction for burnup was around 6%. Neutron self-absorption corrections are calculated and applied to the neutron activation cross sections prior to spectral adjustment described later. The saturated reaction rates are listed in Table 4.

**Table 3.** Correction Factors

| Reaction | Atomic Weight | Isotopic Abundance | Irradiation History | Gamma Absorption | Neutron Burnup | |
|---|---|---|---|---|---|---|
| | | | | | Min | Max |
| 93Nb(n,g)94Nb | 92.906 | 1 | 9.781E-5 | 0.987 | 0.945 | 0.964 |
| 58Fe(n,g)59Fe | 55.845 | 0.00282 | 1.1137 | 0.990 | 0.987 | 0.993 |
| 59Co(n,g)60Co | 58.933 | 0.01* | 0.3152 | 0.997 | 0.913 | 0.942 |
| 54Fe(n,p)54Mn | 55.845 | 0.05845 | 0.9225 | 0.989 | >0.999 | >0.999 |
| 93Nb(n,n')93mNb | 92.906 | 1 | 0.11598 | 1 | >0.999 | >0.999 |

*Fraction of cobalt in the aluminum alloy

**Table 4.** Saturated Reaction Rates in atom/atom-second (1-sigma uncertainties are listed)

| Capsule | $^{54}$Fe(n,p)$^{54}$Mn | | $^{58}$Fe(n,g)$^{59}$Fe | | $^{59}$Co(n,g)$^{60}$Co | |
|---|---|---|---|---|---|---|
| 2 | 1.93E-12 | ±4.2% | 9.82E-11 | ±26.8% | 2.63E-9 | ±4.4% |
| 3 | 2.13E-12 | ±4.2% | 1.30E-10 | ±22.1% | * | |
| 4 | 1.93E-12 | ±3.4% | 1.01E-10 | ±25.0% | 3.17E-9 | ±4.4% |
| 5 | 2.02E-12 | ±4.2% | 1.08E-10 | ±26.0% | * | |
| 6 | 1.35E-12 | ±3.4% | 7.12E-11 | ±21.0% | 2.07E-9 | ±1.2% |

*Not received for analysis

**Table 4**. Saturated Reaction Rates in atom/atom-second (1-sigma uncertainties are listed) Continued

| Capsule | $^{93}Nb(n,g)^{94}Nb$ | | $^{93}Nb(n,n')^{93m}Nb$ | |
|---------|-----------|--------|-----------|--------|
| 2 | 1.28E-10 | ±2.4% | 4.74E-12 | ±5.3% |
| 3 | 1.41E-10 | ±2.4% | 5.32E-12 | ±5.3% |
| 4 | 1.41E-10 | ±2.4% | 5.10E-12 | ±4.8% |
| 5 | 1.25E-10 | ±2.4% | 4.96E-12 | ±4.8% |
| 6 | 9.14E-11 | ±2.5% | 3.73E-12 | ±5.3% |

**Thermal Fluence Adjustments to the Irradiation History**

The irradiation history corrections listed in Table 3 did not take into account the depression of the thermal neutron flux during the early irradiation cycles in the ATR due to the presence of boron (B-10) in the graphite. Calculations of the neutron flux for each cycle show that the thermal neutron flux was depressed about a factor of 3 for the first cycle, 138B, compared to later cycles. Due to the relatively high thermal neutron flux in the ATR, most of the B-10 burns out quickly in the first 5 or 6 reactor cycles such that the thermal flux depression is nearly absent at approximately half-way during the irradiation history. This thermal flux depression has a significant impact on the irradiation history corrections, especially for the $^{58}Fe(n,g)^{59}Fe$ reaction which has the shortest half-life of 44.5 days of the three reactions that were used that are sensitive to thermal neutrons. A simple model was used to take this effect into account. For each cycle, the calculated neutron spectra were characterized by three terms, namely the thermal, epithermal, and fast neutron fluences. The three thermal reaction rates were then approximated as the sum of the thermal flux times the thermal neutron cross section plus the epithermal flux parameter times the resonance integral. The calculated thermal and epithermal neutron fluxes were then used to determine the cycle-dependent reaction rate and normalized to a value of 1 for the last cycle, 145A. However, the normalization appears to have little effect because all of the B-10 has been burned out. The calculations show that the reaction rates for the $^{93}Nb(n,g)$, $^{59}Co(n,g)$, and $^{58}Fe(n,g)$ reactions increase by factors of 1.53, 2.15, and 2.48, respectively, from the first cycle, 138B, to the last cycle, 145A.

The calculated reaction rates for each of the three thermal neutron reactions listed above were multiplied times the time-dependent reactor power to determine a modified irradiation history correction for each reaction separately. The modified irradiation history corrections were 9.845E-5, 0.32393, and 1.391 for the $^{93}Nb(n,g)$, $^{59}Co(n,g)$, and $^{58}Fe(n,g)$ reactions, respectively. By comparison with the values in Table 3, the net effect is shown to reduce the saturated reaction rates in Table 4. For the $^{93}Nb(n,g)^{94}Nb$ reaction, the reduction is only a factor of 1.006 and for the $^{59}Co(n,g)^{60}Co$ reaction the reduction is a factor of 1.028. This result is understandable since

the half-lives of these reactions are much longer than the total length of the irradiation history such that the reactions tend to reflect the net neutron exposure in any case. However, for the $^{58}Fe(n,g)^{59}Fe$ reaction, the saturated reaction rates are reduced by a factor of 1.249. It makes sense that this reaction would have the largest effect since in this case the half-life of $^{59}Fe$ of 44.5 days is much less than the total irradiation time such that the measured activities are higher than expected from a steady state irradiation since they are mainly due to the later reactor cycles where the B-10 effect is no longer significant. The reaction rates in Table 4 were reduced by these factors for all subsequent neutron fluence calculations.

**Neutron Spectral Adjustment**

The STAY'SL [1] computer code was used to adjust the neutron energy spectrum at each location using the calculated reaction rates and uncertainties as input. A time-averaged neutron spectrum that takes into account the thermal flux depression from $^{10}B$ and cycle-dependent effects was provided by staff at INL. . STAY'SL performs a least-squares adjustment to determine the most likely neutron spectrum at each capsule taking into account the uncertainties and covariances of all of the input data (activation data, neutron cross sections, and neutron flux spectra). The neutron activation cross sections and covariances were taken from the International Reactor Dosimetry File, IRDF2002 [2].

Calculations with STAY'SL indicate good agreement with the initial neutron spectra provided by INL. The adjusted neutron fluences from STAY'SL are listed in Table 5 and are shown in Figure 1. To facilitate comparison with neutron spectral calculations at INL, several different energy ranges were used. The thermal fluence is reported including all neutrons < 0.5 eV and < 1.0 eV, The epithermal neutron fluence is listed with energy ranges of 0.5 eV to 0.11 MeV and for 1.0 eV to 0.18 MeV. The fast neutron fluences are listed for thresholds of 0.10 MeV, 0.18 MeV and 1 MeV. A typical neutron spectral adjustment is shown in Figure 2 for capsule 4. The initial STAY'SL adjustments resulted in good agreement for all the neutron activation reactions except for $^{58}Fe(n,g)^{59}Fe$. Poorer agreement for this reaction is explained by the high counting uncertainties as well as uncertainties due to the irradiation history taking into account the relatively short half-life of 44.5 days compared to the length of the irradiation. Taking into account the impact of the $^{10}B$ in the graphite on the thermal neutron flux in the early reactor cycles, as discussed in the previous section of this report, corrects this problem and brings the $^{58}Fe(n,g)^{59}Fe$ reaction rates into very good agreement with the other two thermal neutron reaction rates.

The initial neutron spectra used for the spectral adjustments with STAY'SL in the prior versions of this report used the neutron spectrum from cycle 142A provided by INL since this was about mid-way through the irradiation cycle. Due to the large thermal flux depression from B-10 in the graphite during the early cycles, INL provided a neutron spectrum that was time-averaged over the entire irradiation history. This time-averaged neutron spectrum was used for the neutron spectral adjustments in this revision of the report, as shown in Figure 2.

## Radiation Damage Calculations

The adjusted neutron spectra for all three capsules, as illustrated in Figure 1, were used to calculate radiation damage parameters using the SPECTER computer code [3]. Displacement per atom (dpa) for several important elements and Type 304 stainless steel are listed in Table 6. The stainless steel dpa values include the small additional contribution from Ni-59 reactions [4].

**Table 5.** Adjusted Neutron Fluences

| | Thermal* | | Epithermal | | Fast | | Fast | |
|---|---|---|---|---|---|---|---|---|
| | < 0.5 eV | | 0.5 eV to 0.11 MeV | | > 0.10 MeV | | > 0.18 MeV | |
| Capsule | n/cm$^2$ | ±% | n/cm$^2$ | ±% | n/cm$^2$ | ±% | n/cm$^2$ | ±% |
| 2 | 4.39e+21 | 13 | 5.49e+21 | 16 | 3.65e+21 | 8 | 3.19e+21 | 7 |
| 3 | 5.19e+21 | 16 | 5.55e+21 | 15 | 3.81e+21 | 8 | 3.33e+21 | 7 |
| 4 | 5.25e+21 | 14 | 5.56e+21 | 16 | 3.72e+21 | 8 | 3.25e+21 | 7 |
| 5 | 4.52e+21 | 10 | 4.97e+21 | 13 | 3.49e+21 | 8 | 3.06e+21 | 7 |
| 6 | 3.46e+21 | 13 | 3.63e+21 | 16 | 2.65e+21 | 8 | 2.33e+21 | 7 |

*Thermal fluence is defined as the sum of all neutrons < 0.5 eV.

| | Thermal* | | Epithermal | | Fast | |
|---|---|---|---|---|---|---|
| | < 1.0 eV | | 1.0 eV to 0.18 MeV | | > 1 MeV | |
| Capsule | n/cm$^2$ | ±% | n/cm$^2$ | ±% | n/cm$^2$ | ±% |
| 2 | 4.63e+21 | 13 | 5.63e+21 | 16 | 1.41e+21 | 5 |
| 3 | 5.47e+21 | 16 | 5.67e+21 | 15 | 1.48e+21 | 5 |
| 4 | 5.54e+21 | 14 | 5.68e+21 | 16 | 1.43e+21 | 5 |
| 5 | 4.77e+21 | 10 | 5.09e+21 | 13 | 1.38e+21 | 5 |
| 6 | 3.64e+21 | 13 | 3.71e+21 | 16 | 1.04e+21 | 5 |

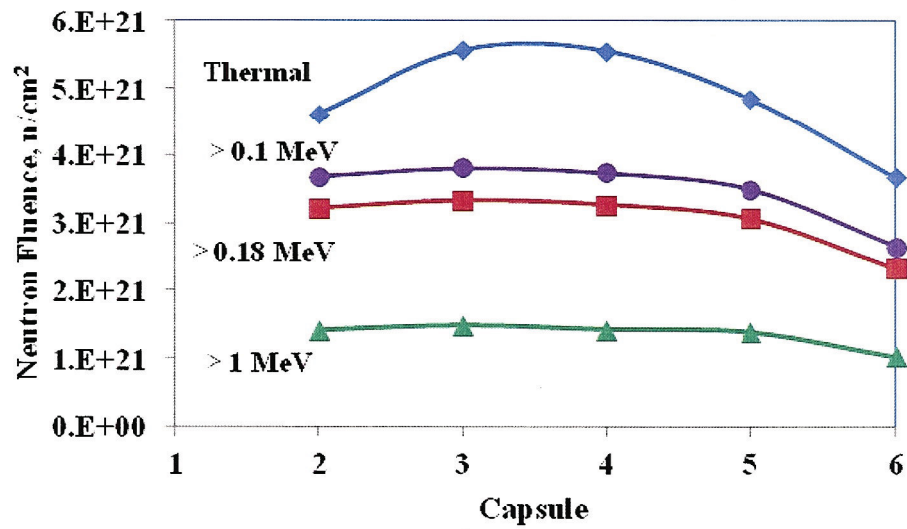*Thermal fluence is defined as the sum of all neutrons < 1.0 eV.

**Figure 1.** Neutron fluence values for capsules in the AGR-1 assembly
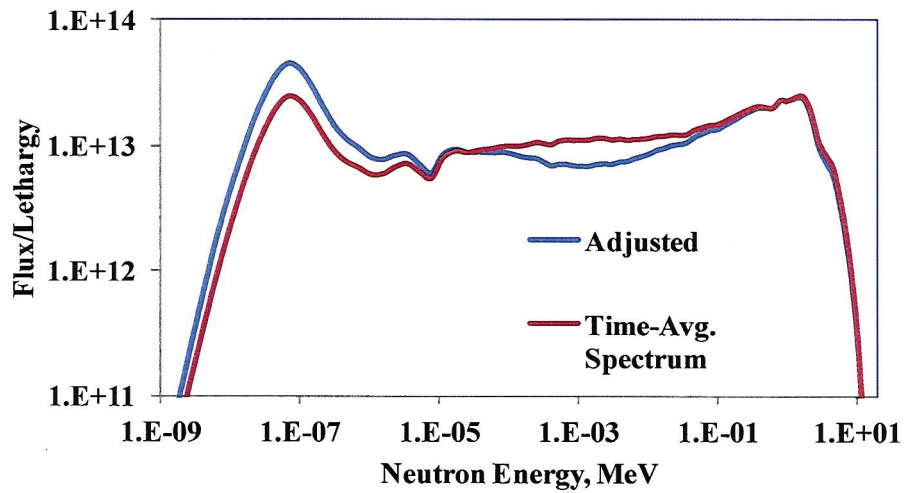


**Figure 2.** Adjusted Neutron Flux Spectrum for Capsule 4

**Table 6.** Calculated DPA Values for the AGR-1 Irradiation Capsules

| Element | Capsule 2 | Capsule 3 | Capsule 4 | Capsule 5 | Capsule 6 |
|---------|-----------|-----------|-----------|-----------|-----------|
| C | 2.67 | 2.75 | 2.70 | 2.52 | 1.92 |
| Al | 4.33 | 4.49 | 4.39 | 4.14 | 3.14 |
| Cr | 2.45 | 2.57 | 2.49 | 2.37 | 1.77 |
| Mn | 2.79 | 2.91 | 2.84 | 2.68 | 2.01 |
| Fe | 2.17 | 2.27 | 2.20 | 2.10 | 1.57 |
| Ni* | 2.82 | 3.07 | 3.00 | 2.75 | 1.99 |
| 304SS** | 2.30 | 2.42 | 2.35 | 2.23 | 1.66 |

\* Includes additional dpa from thermal neutron $^{59}$Ni reactions

\*\*Type 304 stainless steel – Fe (0.70) Cr (0.18) Ni (0.10) Mn (0.02)

**Melt Wire Monitors**

Vanadium melt wire monitors containing two Be wires were irradiated in each AGR-1 capsule (Table 1, above). Following disassembly at INL, PNNL received monitors that were recovered from capsules 2, 4, and 6 and the graphite cores from capsules 1 and 5. The melt wires could not be recovered from capsule 3. Since Be does not have any distinct gamma-emitting activation products, it was not possible to uniquely confirm the identification of the monitors by gamma counting. All monitors and other materials were opened for examination in a fume hood at PNNL. Individual items from each monitor were individually examined under a microscope and pictures were recorded for documentation (attached). Several of the items were determined to be niobium gas lines using microscopic examination and confirmed by gamma counting which showed the presence of significant $^{94}$Nb activity. The experimental plan was to locate and identify the melt wire monitors and then open them to see if the Be wires melted or not. This was not possible because all of the monitors that were retrieved were broken and only parts of the capsules were found. Attempts to positively identify monitors by the laser etch ID on the side were not successful due to the very poor condition of the monitors. It is thought that the poor condition of the monitors is explained by partial carburization due to reactions between the vanadium and graphite at elevated temperature during the irradiation. However, pictures of the items that were identified as melt wire monitors had the same appearance as the unirradiated melt wire monitors such that it was concluded that parts of melt wire monitors were located and

examined in capsules 2, 4, and 6. Detailed notes and pictures are presented below for each capsule.

Capsule 1: PNNL received a graphite core for disassembly. The graphite was placed in a plastic bag (used to control the spread of contamination) and small pliers were used to break the graphite in an attempt to locate the melt wire monitors. Unfortunately, nothing resembling a melt wire monitor was located after complete disintegration of the graphite core, as shown in Picture 1.

Capsule 2: Six pieces were received for analysis. Gamma spectroscopy of the pieces showed that most contained $^{60}$Co, $^{54}$Mn, and $^{110m}$Ag which would be compatible with pieces of graphite used for spacers. Microscopic examination showed that one of the pieces appeared to be a melt wire capsule with one end broken off. The welded end was then cut off and the monitor broke in half as shown in Picture 2. The welded end of the monitor contains a metallic gray mass which is most likely the residue of the melted Be wires. The inner walls of the monitor also appear to be the same gray color which is most likely due to melted Be. The conclusion is that the Be wires melted and the residue was found in the welded end and coating the walls of the monitor.

Capsule 3: The melt wire package broke up during disassembly at INL and was not retrieved.

Capsule 4: A piece of what was believed to be the melt wire package was examined at PNNL. Microscopic examination shows that the item appears to be part of the melt wire monitor. The welded end of the monitor was cut off and Picture 3 shows what appears to be the residue of the Be melt wires. The conclusion is that the Be wires melted and the residue settled in the welded end.

Capsule 5: PNNL received a graphite core thought to contain the melt wire monitor. The graphite core was placed in a plastic bag and pliers were used to break the core up in an attempt to recover the monitor. Two cylindrical rods were retrieved. However, microscopic examination as shown in Picture 4 illustrates that these rods are graphite inserts, not the melt wire monitor. Nothing else resembling the appearance of the monitor could be located. It is not clear why this was the case since the melt wire monitor was positioned deeper in the core than the graphite inserts. Picture 4 shows the remainder of the graphite core after removal of the two graphite inserts.

Capsule 6: PNNL received three "flux wire" packages and what was thought to be the "melt wire" package. Gamma counting showed that one of the "flux wire" packages had no significant activity and the "melt wire" package was determined to be the iron flux wire monitor broken in two parts. Microscopic examination of the remaining item showed that it appeared to be the melt wire monitor, as shown in Picture 5. The monitor was cut open in an attempt to see if the melt wires melted. However, the appearance of the inside of the monitor is very shiny and does not have the gray metallic look that would be expected for Be, as was found for capsules 2 and 4. The monitor was broken and the welded end was not recovered. For capsules 2 and 4, the melted

Be was found in the welded end of the monitor. The orientation of the melt wire monitor in capsule 6 is not known; however, if it were the same as for capsules 2 and 4, then melted Be would have been in the welded end that was not recovered. Consequently, we cannot determine if the Be wires melted or not since the monitor was broken and there was no evidence for melted Be on the part of the monitor that was examined.

**References**

[1] F. G. Perey, Least Squares Dosimetry Unfolding: The Program STAY'SL, ORNL/TM-6062 (1977).

[2] International Reactor Dosimetry File 2002 (IRDF-2002), IAEA Technical Reports Series No. 452, International Atomic Energy Agency, Vienna, Austria, November 2006.

[3] L. R. Greenwood and R. K. Smither, SPECTER: Neutron Damage Calculations for Materials Irradiations, ANL/FPP-TM-197, January 1985.

[4] L. R. Greenwood, A New Calculation of Thermal Neutron Damage and Helium Production in Nickel, Journal of Nuclear Materials 115 (1983) 137-142.

Picture 1 – Remains of graphite core from capsule 1.  The melt wire monitor could not be located.
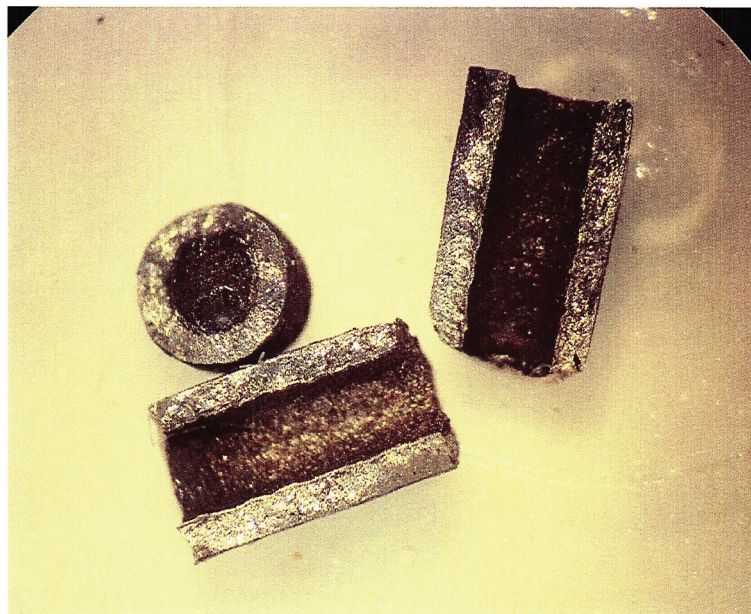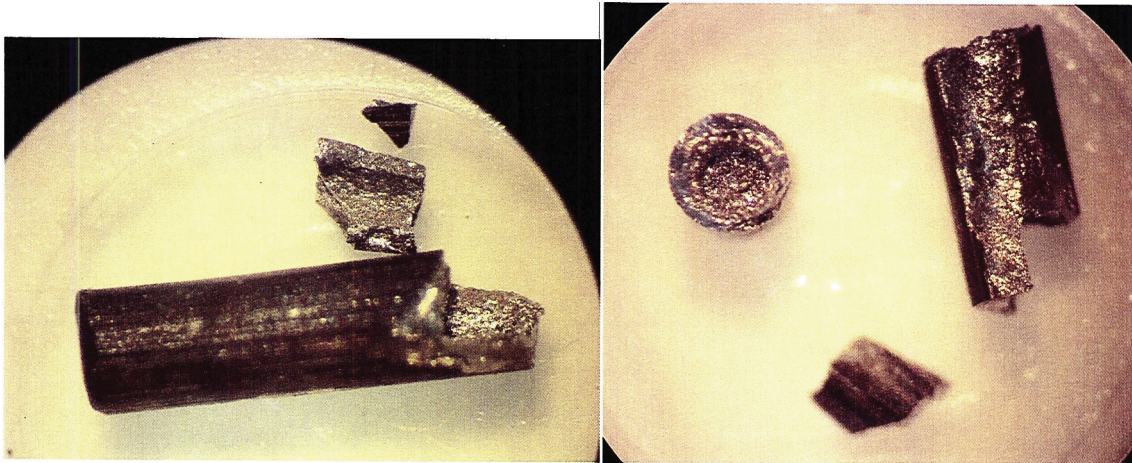


Picture 2 – Melt wire monitor capsule 2.  The gray metallic mass in the welded end cap and gray inner walls are thought to be the residue of the melted Be wires.
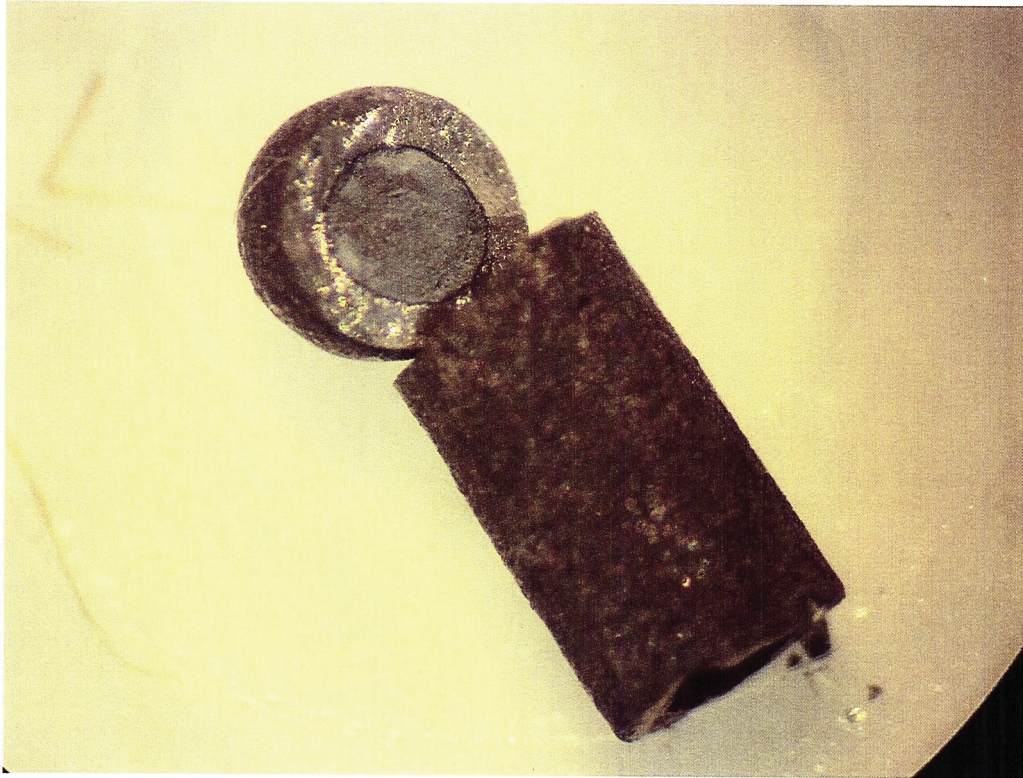
Picture 3 – Broken melt wire monitor from capsule 4.  The gray metallic mass in the welded end cap is thought to be the residue of the melted Be wires.
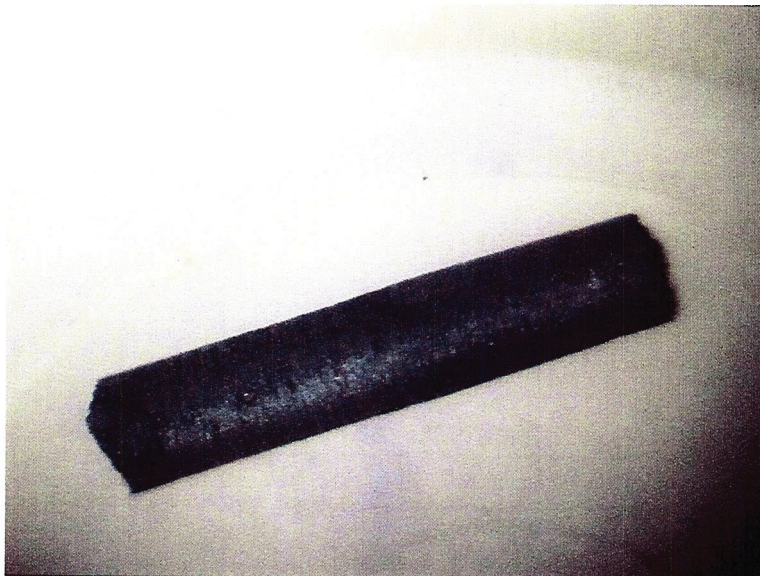


Picture 4 – Graphite insert removed from graphite core retrieved from capsule 5.  No melt wire monitor could be located.

Picture 5 – Pictures of the melt wire monitor retrieved from capsule 6. The inside of the capsule and cut off welded end is highly reflective and not consistent with the gray metallic appearance expected for Be and as seen in the pictures of capsules 2 and 4.